Validation of MODIS aerosol optical depth retrieval over land

D. A. Chu,[1,2] Y. J. Kaufman,[2] C. Ichoku,[1,2] L. A. Remer,[2] D. Tanré,[3] and B. N Holben[4]

[1] Aerosol optical depths (τ_a) are derived operationally for the first time from the MODIS (Moderate Resolution Imaging Spectroradiometer) measurements over vegetated and partially vegetated land at 0.47 and 0.66 μm wavelengths. The extensive validation made during July – September 2000 encompasses 315 co-located τ_a in space and time derived by MODIS and AERONET (Aerosol Robotic Network) from more than 30 AERONET sites. The lack of AERONET measurements in East Asia, India and Australia makes this validation unavailable for those regions. The MODIS aerosol retrievals, except in coastal zones, are found within the retrieval errors of $\Delta\tau_a = \pm0.05 \pm0.2 \tau_a$. The root mean square (RMS) errors are ≤ 0.1 in the continental inland regions and up to 0.3 in the coastal regions (attributed mainly to water contaminated signals). With this validation we believe that MODIS aerosol products can be used quantitatively in many applications with caution for possible residual clouds, snow/ice, and water contamination. *INDEX TERMS:* 1610 Global Change: Atmosphere (0315, 0325); 1640 Global Change: Remote sensing; 3360 Meteorology and Atmospheric Dynamics: Remote sensing

1. Introduction

[2] The application of satellite data to derive global aerosol properties has advanced dramatically in the last few years [*King et al.*, 1999]. One of the main advancements is the systematic derivation of aerosol over land from MODIS onboard the EOS-Terra satellite launched on December 18, 1999. Since February 24, 2000, MODIS has continuously acquired daily global measurements with thirty-six spectral bands (0.41 – 14 μm) at three different spatial resolutions (250 m, 500 m and 1 km) [*Salomonson et al.*, 1989]. We retrieve aerosol properties over both land [*Kaufman et al.*, 1997a] and ocean [*Tanré et al.*, 1997] using seven well calibrated spectral channels in the solar spectrum (0.47 – 2.1 μm). In this paper we present the first comprehensive validation of the MODIS-derived τ_a over land.

[3] The MODIS retrieval of τ_a over land employs primarily three spectral channels centered at 0.47, 0.66, and 2.1 μm wavelength at 500m resolution. A short description of the MODIS aerosol algorithm presented here follows *Kaufman et al.* [1997a]. In a 10 km × 10 km grid box, cloud-free pixels are first selected using the multi-spectral MODIS cloud mask [*Ackerman et al.*, 1998]. The cloud mask uses more than twenty tests, including two cirrus detection tests, to indicate a cloudy or clear pixel at 1 × 1 km resolution. Fine-mode aerosols are transparent at 2.1 μm wavelength, allowing the direct observation of land surface. The empirical relationships developed over vegetated surfaces are used to estimate the surface reflectance (ρ_s) at 0.47 μm and at 0.66 μm from the measurements at 2.1 μm ($\rho_s^{0.47\mu m}/\rho_s^{2.1\mu m} = 0.25$ and $\rho_s^{0.66\mu m}/\rho_s^{2.1\mu m} = 0.5$) [*Kaufman et al.*, 1997b]. To minimize the error, the MODIS aerosol retrievals over land are limited to pixels of $\rho_s^{2.1\mu m} < 0.15$. Snow/ice and water covered surfaces are excluded because the empirical relationships given above are invalid over those regions. The selected cloud-free dark pixels in the grid box may still be partially contaminated by sub-pixel clouds, snow/ice, or soil types that do not fit the empirical relationship (e.g., red soil [*Gatebe et al.*, 2001]). Thus only the 10–40 percentile of MODIS measured radiance is used. The overall retrieval errors were estimated to be $\Delta\tau_a = \pm0.05 \pm 0.2\tau_a$ (~100% error for $\tau_a = 0.05$). Larger error of ±0.3 is found for dust particles when using the 2.1 μm channel [*Kaufman et al.*, 2000] as opposed to ±0.05 for urban/industrial and biomass burning aerosols. To distinguish between dust and non-dust aerosols, the ratio of aerosol path radiance at 0.66 and 0.47 μm is used. Sulfate and smoke aerosols that cannot be distinguished by the path radiance ratio are separated a priori according to the geographic locations and seasons of their emission sources. The details of the determination of aerosol types (including the mixture of different aerosols) and the aerosol models used by the retrieval algorithm can be found in *Kaufman et al.* [1997a].

[4] The release of MODIS level-2 (10 km × 10 km) granule-based (granule: a 5-minute segment of one MODIS orbital data) aerosol products in August 2000 and later level-3 (1° × 1°) gridded products was to provide a preview before quality assurance. The validation data presented here are the basis for the release of the first version of validated products.

2. Validation Approach

[5] In order to take into account both spatial and temporal variabilities of aerosol distribution, the MODIS retrievals at 10 km × 10 km resolution and the AERONET direct Sun measurements at 15-minute intervals [*Holben et al.*, 1998] need to be co-located

[1]Science Systems and Applications Inc., Lanham, Maryland, USA.
[2]Laboratory for Atmospheres, NASA Goddard Space Flight Center, Greenbelt, Maryland, USA.
[3]Laboratorire d'Optique Atmospherique, Universite des Sciences et Technologies de Lille, Villeneuve d'Ascq, France.
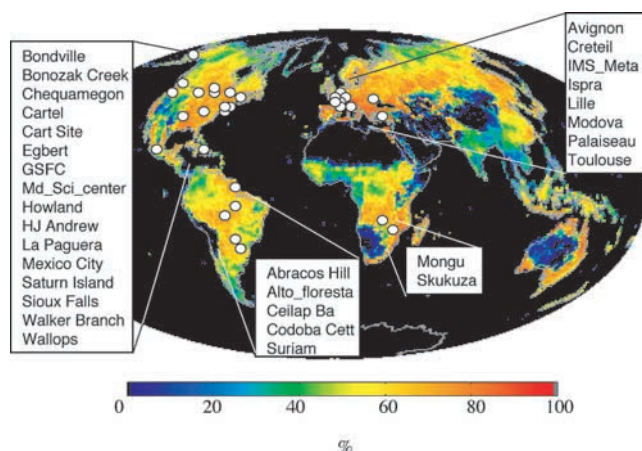[4]Laboratory for Terrestrial Physics, NASA Goddard Space Flight Center, Greenbelt, Maryland, USA.
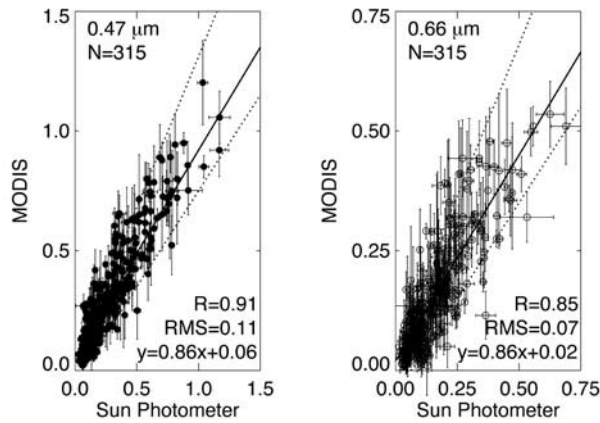
Figure 1. Frequency map of MODIS aerosol retrievals over land derived from MODIS 1° × 1° level-3 daily products between July and September 2000. The white circles depict the locations of AERONET Sun photometer sites.

Figure 2. Global comparisons of MODIS- and AERONET-derived τ_a at 0.47 and 0.66 µm wavelengths, encompassing 315 points from more than 30 AERONET sites excluding Venice and El Arenosillo coastal sites. The solid lines represent the slopes of linear regression and the dot lines the retrieval errors of $\Delta\tau_a = \pm0.05 \pm 0.2\tau_a$. Temporal and spatial standard deviations are shown as the error bars in x(AERONET)- and y(MODIS)-direction respectively.

in space and time. We require at least 2 out of possible 5 AERONET measurements within ±30 min of MODIS overpasses and at least 5 out of possible 25 MODIS retrievals in a square box of 50 km × 50 km centered over AERONET sites. The mean values of the co-located spatial and temporal ensemble are then used in linear regression analysis and in calculating RMS errors. The AERONET level 1.5 data are cloud screened. Though the level 2.0 data provide final calibration, they are not available in real time. Therefore, the

level 1.5 data (instead of level 2.0) are used in the operational MODIS aerosol validation scheme [*Ichoku et al.*, 2002].

3. Validation of Aerosol Optical Depth

[6] Figure 1 displays the frequency map of MODIS aerosol retrievals over land as derived using the level-3 daily aerosol products from July to September 2000. Superimposed are the locations of the AERONET sites included in this validation. The MODIS aerosol retrievals cover approximately 70% of the land surface. The frequency lower than 100% of a given $1° \times 1°$ grid box is due to cloud cover, non-vegetated surfaces, or missing data. Most of the regions with dust occurrence are excluded due to high brightness of desert surface (e.g., the Sahara Desert). Also excluded are snow/ice-covered regions (e.g., Antarctica and Greenland)—too bright in the visible wavelength to derive aerosol optical depth. At high latitudes, more retrievals are seen because of the overlapped satellite orbits.

[7] A total of 315 points representing more than 30 AERONET sites meet our match-up criteria for the MODIS- and AERONET-derived τ_a in the period of July – September 2000. Small islands, such as Barbados, Bermuda, Cape Verde, Hawaii, etc., are too small for aerosol land validation. The slopes (S_l) of linear regression represent systematic biases if differing from 1 and the intercepts (I_c) represent the errors in the ρ_s estimates. Large errors in ρ_s lead to large I_c. The scatter plots in Figures 2a and 2b depict overall a very good agreement between MODIS and AERONET with $S_l \sim 0.86$, $I_c \sim 0.02-0.06$, and high correlation coefficients (R) $\sim 0.85-0.91$. Nearly all the points fall within the retrieval errors of $\Delta\tau_a = \pm0.05 \pm 0.2\tau_a$ with RMS errors ranging from 0.07 to 0.11. Venice and El Arenosillo coastal sites excluded in Figure 2 with larger RMS errors ($\sim 0.2-0.3$) and I_c (~ 0.2) will be discussed later. The systematic biases in MODIS retrievals are mainly due to aerosol model assumptions (deviation of $0-20\%$), instrument calibration ($2-5\%$), or the choice of the lowest 10–40 percentile
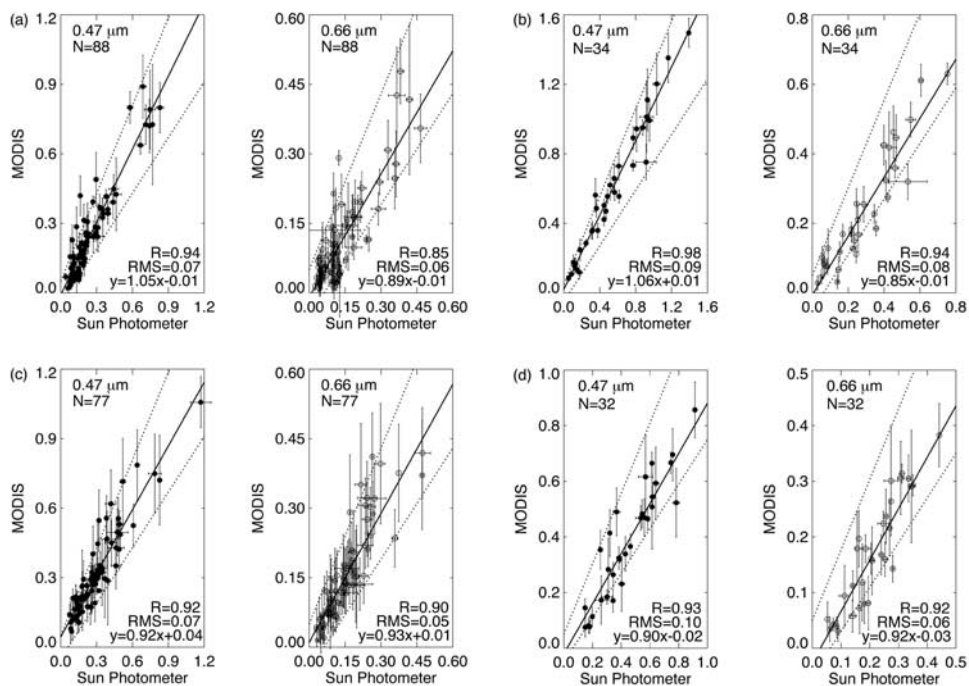

Figure 3. Regional comparisons of MODIS- and AERONET-derived τ_a at 0.47 and 0.66 µm wavelengths in the continental inland regions: (a) eastern US, (b) Brazil, (c) western Europe, and (d) southern Africa. The solid lines represent the slopes of linear regression and the dot lines the retrieval errors of $\Delta\tau_a = \pm0.05 \pm 0.2\tau_a$. Temporal and spatial standard deviations are shown as the error bars in x(AERONET)- and y(MODIS)-direction respectively.

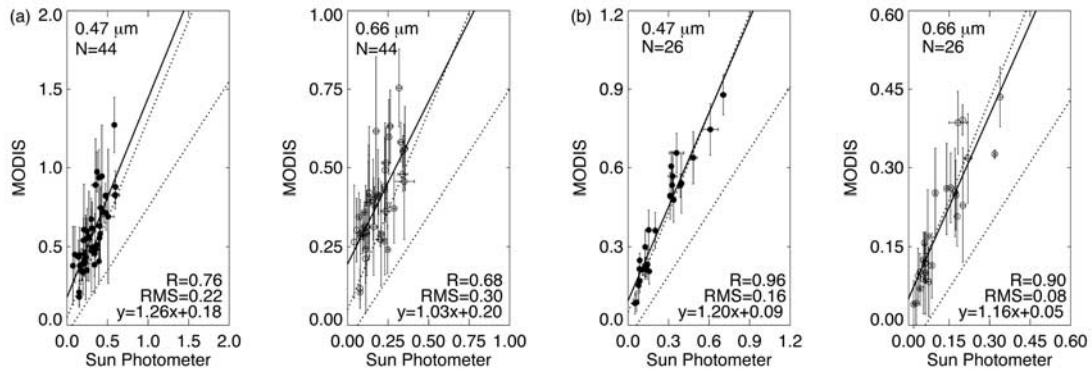**Figure 4.** Same as in Figure 3 except for the continental coastal zones: (a) Venice and El Arenosillo and (b) NASA GSFC, Wallops, and Maryland Science Center.

of the measurements (0–10%). In the following subsections, we examine two regions in detail: (1) the continental inland regions of eastern US and western Europe, Brazil and southern Africa, for the similar occurrence of the industrial/urban pollution and biomass burning aerosols, and (2) the continental coasts of the eastern US and western Europe for the effect of water contamination.

3.1 Continental Inland

[8] Figures 3a and 3b show the comparisons between the MODIS- and AERONET-derived τ_a in the eastern US and in Brazil where pre-launch field experiments took place with dominant urban/industrial and biomass burning aerosols, respectively. The small values of $I_c \sim 0.01$ in Figures 3a and 3b reveal that the vegetated surfaces, such as evergreen, deciduous, mixed forests, and cropland, give the best estimates of ρ_s as anticipated. In terms of S_l, smaller deviations from unity are found at 0.47 μm (≤ 0.05) than at 0.66 μm (>0.1). The S_l of 0.86 in Figure 3b is unexpected because it disagrees with previous validation. The single scattering albedo (ω_o) of 0.90 was shown to result in the best fit of τ_a ($S_l \sim 0.97$, $I_c \sim 0.03$, $R \sim 0.98$) derived from MODIS Airborne Simulator and AERONET measurements [*Chu et al.*, 1998]. We assumed the same ω_o (=0.90) at 0.47 and 0.66 μm despite the recent work of *Dubovik et al.* [2000] that ω_o may be slightly higher at 0.47 μm than at 0.66 μm. The difference, however, is not significant. Interannual variation in aerosol properties and stronger

calibration drift of AERONET Sun photometers at 0.66 μm [Smirnov et al., personal communication] are suspected to be the primary reasons for producing the poorer fit.

[9] The MODIS retrievals in regions with urban/industrial pollution or smoke from biomass burning are based on the aerosol models derived from field measurements in the eastern US and in Brazil. The similar S_l and I_c shown in Figures 3a and 3c imply that the differences, if any, in aerosol particle size and chemical composition are too small to affect the retrievals. For biomass burning aerosol, the values of S_l deviating from 1 (0.1 at 0.47 μm and 0.08 at 0.66 μm) in Figure 3d are most likely caused by higher
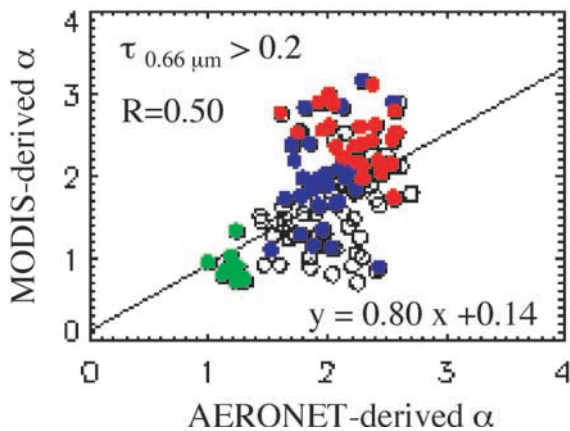

Figure 5. Comparison of MODIS and AERONET-derived α when $\tau_a^{0.66\mu m} > 0.2$ (red: biomass-burning aerosol; blue: industrial/urban aerosol with dust particle; white: biomass-burning or urban/industrial aerosols outside the regions as shown in Figure 3).
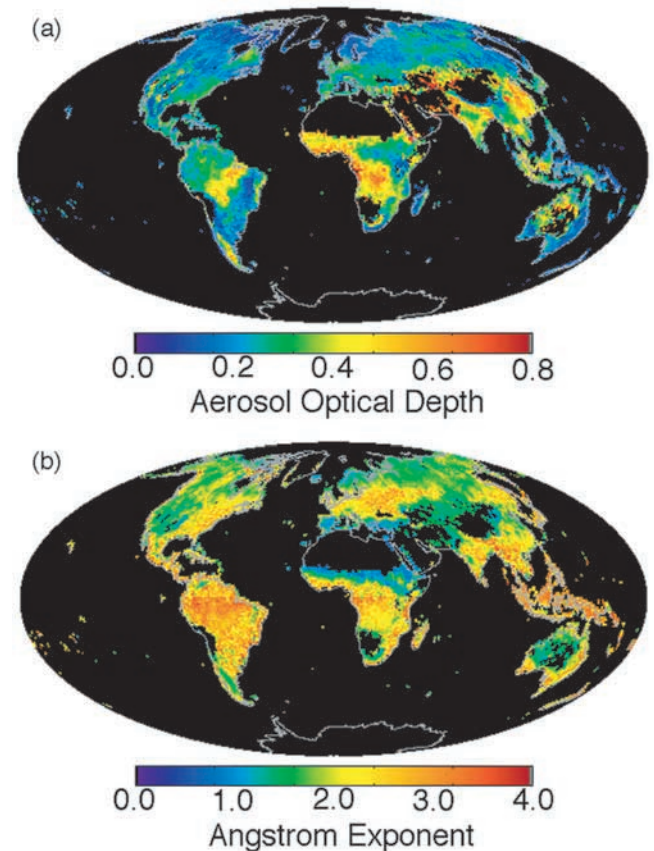
Figure 6. Global monthly mean of (a) τ_a (at 0.55 μm) and (b) α derived from MODIS 1° × 1° level-3 daily products of September 2000.

soot concentration from the biomass burning in southern Africa than in South America. In other words, lowering ω_o will result in a better fit, which is in agreement with the ω_o values (smaller ω_o in southern Africa than in South America) derived by *Dubovik et al.* [2000].

3.2. Continental Coasts

[10] Surface inhomogeneity or sub-pixel water contamination has a larger effect than we anticipated in continental coastal regions. We examined five AERONET sites: NASA GSFC (US), Maryland Science Center (US), Wallops (US), Venice (Italy), and El Arenosillo (Spain). Clearly, the values of $I_c \sim 0.18$ and 0.2 derived at Venice and El Arenosillo are twice larger than those of 0.05 and 0.09 derived at the US coastal sites (see Figures 4a and 4b). The large RMS errors ($\sim 0.20-0.30$) are closely associated with the large intercepts ($\sim 0.18-0.2$). The smaller values of I_c (< 0.1) resulting from the US east coast in July–September (usually dry) are in contrast to earlier results ($\sim 0.15-0.2$) in spring (usually wet) caused by standing water from frequent rain events.

4. Spectral Dependence of Aerosol Optical Depth

[11] Ångström exponent (α) is commonly used to describe the spectral dependence of τ_a. For MODIS, α is calculated as follows

$$\alpha = -ln(\tau_a^{0.47\mu m}/\tau_a^{0.66\mu m})/ln(0.47/0.66)$$

where $\tau_a^{0.47\mu m}$ and $\tau_a^{0.66\mu m}$ are the MODIS-derived τ_a at 0.47 μm and 0.66 μm, respectively. The uncertainty in surface reflectance is shown to be one of the important factors in the derivation of α. A reasonable fit ($S_l \sim 0.80$, $I_c \sim 0.14$, $R \sim 0.50$) is found between MODIS- and AERONET-α when $\tau_a^{0.66\mu m} > 0.2$ because of the diminishing effect of the error in surface reflectance estimates (see Figure 5). Other factors affecting the accuracy of α include the uncertainties of aerosol properties, e.g, ω_o and particle size.

5. Aerosol Global Distribution

[12] The global monthly means of τ_a and α over land are shown in Figures 6a and 6b for September 2000, respectively. We select the month of September because there are more complete data in that month than in July or August. The dry-season biomass burning in Africa and in South America is most visible with mean optical depths $\sim 0.5-0.7$ compared to the air pollution in Europe and North America with means $\sim 0.2-0.3$ and in China and India with means $\sim 0.4-0.5$. The corresponding α values reveal reasonable correlation with urban/industrial aerosol in North America, Europe, China, and India, and with biomass-burning aerosol in Brazil and southern Africa. Slightly small α values at the boundary of the Sahara Desert show possible mixture of urban/industrial or biomass burning aerosols with dust particles.

6. Concluding Remarks

[13] The MODIS aerosol retrievals over land meet our expectation with unprecedented accuracy. With the continuous refine-ments in instrument calibration, we expect the quality of MODIS aerosol products to be improved with time. However, several sources of the errors in aerosol retrieval remain to be solved, such as sub-pixel cloud, snow/ice, and water contamination, uncertainties in heterogeneous surface reflectance, and aerosol properties beyond the scope of the assumptions of aerosol models. The scenarios of dust outbreaks and air pollution in East Asia are good test beds for testing the surface reflectance estimation and aerosol models. The ACE-Asia field campaign taking place in March–May 2001 shall provide important insight for evaluating MODIS aerosol retrievals in that region.

References

Ackerman, S. A., et al., Discriminating clear-sky from clouds with MODIS, *J. Geophys. Res.*, *103*, 32,141–32,158, 1998.

Chu, D. A., et al., Remote sensing of smoke from MODIS airborne simulator during SCAR-B experiment, *J. Geophys. Res.*, *103*, 31,979–31,987, 1998.

Dubovik, O., et al., Accuracy assessments of aerosol properties retrieved from AERONET Sun and sky-radiance measurements, *J. Geophys. Res.*, *105*, 9791–9806, 2000.

Gatebe, C. K., et al., Sensitivity of off-nadir zenith angle to correlation between visible and near-infrared reflectance for use in remote sensing of aerosol over land, *IEEE Trans. on Geos. and Remote Sens.*, *39*(4), 805–819, 2001.

Holben, B. N., et al., AERONET—A federated instrument network and data archive for aerosol characterization, *Remote Sens. Environ.*, *66*(1), 1–16, 1998.

Ichoku, C., D. A. Chu, S. Mattoo, et al., A spatio-temporal approach for global validation and analysis of MODIS aerosol products, *Geophys. Res. Lett.*, *29*(12) MOD 1, 1–4, 2002.

King, M. D., et al., Remote sensing of tropospheric aerosols from space: Past, present and future, *Bull. Am. Meteorol. Soc.*, *80*, 2229–2259, 1999.

Kaufman, Y. J., et al., Operational remote sensing of tropospheric aerosol over the land from EOS-MODIS, *J. Geophys. Res.*, *102*, 17,051–17,061, 1997a.

Kaufman, Y. J., et al., The MODIS 2.1 μm channel—Correlation with visible reflectance for use in remote sensing of aerosol, *IEEE Trans. Geos. and Remote Sens.*, *35*(5), 1286–1298, 1997.

Kaufman, Y. J., et al., Detection of dust over the desert by EOS-MODIS, *IEEE Trans. on Geos. and Remote Sens.*, *38*, 525–531, 2000.

Salomonson, V., et al., MODIS Advanced facility instrument for studies of the earth as a system, *IEEE Trans. on Geos. and Remote Sens.*, *27*(2), 145–153, 1989.

Tanré, D., et al., Remote sensing of aerosol over oceans from EOS-MODIS, *J. Geophys. Res.*, *102*, 16,971–16,988, 1997.

———————

D. A. Chu, C. Ichoku, Y. J. Kaufman, and L. A. Remer, Code 913, NASA/Goddard Space Flight Center, Greenbelt, MD 20771, USA. (achu@climate.gsfc.nasa.gov)

D. Tanré, Laboratorire d'Optique Atmospherique, Universite des Sciences et Technologies de Lille, Villeneuve d'Ascq, France. (tanre@loa.univ-lillel.fr)

B. N. Holben, Laboratory for Terrestrial Physics, NASA Goddard Space Flight Center, Greenbelt, Maryland, USA. (brent@aeronet.gsfc.nasa.gov)